Aquifer Thermal Energy Storage (ATES) smart grids

Large-scale seasonal energy storage as a distributed energy management solution

Rostampour, Vahab; Jaxa-Rozen, Marc; Bloemendal, Martin; Kwakkel, Jan; Keviczky, Tamás

DOI
10.1016/j.apenergy.2019.03.110

Publication date
2019

Document Version
Accepted author manuscript

Published in
Applied Energy

Aquifer Thermal Energy Storage (ATES) Smart Grids: Large-Scale Seasonal Energy Storage as A Distributed Energy Management Solution*

Vahab Rostampour[a,+,⋆], Marc Jaxa-Rozen[b,+], Martin Bloemendal[c,d], Jan Kwakkel[b], and Tamás Keviczky[a]

[+]These authors contributed equally to this work
[⋆]Corresponding author: v.rostampour@tudelft.nl
[*]This research was supported by the Uncertainty Reduction in Smart Energy Systems (URSES) research program funded by the Dutch organization for scientific research (NWO) and Shell under the project Aquifer Thermal Energy Storage Smart Grids (ATES-SG) with grant number 408-13-030.
[a]Delft Center for Systems and Control, Delft University of Technology, Mekelweg 2, 2628 CD, Delft, The Netherlands.
[b]Faculty of Technology, Policy and Management, Delft University of Technology, Jaffalaan 5, Delft 2628 BX, The Netherlands
[c]Faculty of Civil Engineering and Geosciences, Delft University of Technology, Stevinweg 1, 2628 CN Delft, The Netherlands
[d]KWR Watercycle Research Institute, Groningenhaven 7, 3433 PE Nieuwegein, The Netherlands

ABSTRACT

Aquifer Thermal Energy Storage (ATES) is a building technology used to seasonally store thermal energy in the subsurface, which can reduce the energy use of larger buildings by more than half. The spatial layout of ATES systems is a key aspect for the technology, as thermal interactions between neighboring systems can degrade system performance. In light of this issue, current planning policies for ATES aim to avoid thermal interactions; however, under such policies, some urban areas already lack space for the further development of ATES, limiting achievable energy savings. We show how information exchange between ATES systems can support the dynamic management of thermal interactions, so that a significantly denser layout can be applied to increase energy savings in a given area without affecting system performance. To illustrate this approach, we simulate a distributed control framework across a range of scenarios for spatial planning and ATES operation in the city center of Utrecht, in The Netherlands. The results indicate that the dynamic management of thermal interactions can improve specific greenhouse gas savings by up to 40% per unit of allocated subsurface volume, for an equivalent level of ATES economic performance. However, taking advantage of this approach will require revised spatial planning policies to allow a denser development of ATES in urban areas.

Introduction

Aquifer Thermal Energy Storage (ATES) is an innovative building technology which can be used on a large scale to store thermal energy in natural subsurface formations. In combination with a heat pump, ATES can reduce energy use for heating and cooling by more than half in larger buildings[1,2], while supporting the electrification of building energy systems. This has made the technology increasingly popular in Northern Europe. For instance, it is currently used in approximately 10% of new commercial and institutional buildings in The Netherlands, where ATES has been identified as a key technology towards long-term targets for greenhouse gas (GHG) emissions reductions in the built environment. Furthermore, the conditions required for ATES are relatively widespread across the globe; by the middle of the century, roughly half of the world's urban population is expected to live in areas with suitable subsurface and climate conditions for ATES[3]. These areas include large parts of China and North America, where the large-scale deployment of ATES could eventually reduce total energy demand for space heating and cooling by up to 10% in large residential, commercial and institutional buildings[4].

However, the progressive adoption of this technology in Europe has already evidenced some issues of concern for policymakers. The spatial layout and planning of ATES systems is a key aspect for the management of the technology, as thermal interferences between neighboring systems which share an aquifer can affect their technical and economic performance. Current regimes for ATES management have therefore followed a highly conservative approach, to minimize the risk of a "tragedy of the commons"[5] – in which the overly dense development of ATES systems could lead to thermal interferences,

and eventually degrade the potential of aquifers for thermal storage. However, recent research suggests that current planning methods are essentially incompatible with long-term objectives for the development of ATES; for instance, several urban areas in the Netherlands already lack the space to accommodate further demand for ATES[6], although the technology's total market share is still only one-fifth of national policy objectives[7]. This situation presents a trade-off between public and private interests: while relaxed planning guidelines could contribute to GHG mitigation efforts by increasing the adoption of ATES, this could reduce the economic performance of the technology – and ultimately its long-term attractiveness as an energy-efficient option for building owners.

Improved methods for the management and operation of ATES systems will therefore be needed to better align the interests of policymakers and building owners, and fulfill the technical potential of ATES. To this end, this paper presents distributed ATES control as a starting point towards an improved regime for the management of ATES in urban areas. This approach enables the dynamic management of thermal interactions in the subsurface – thus allowing a significantly denser spatial layout for ATES without affecting system performance, and increasing feasible energy savings from a given subsurface volume. To illustrate this approach, we develop and simulate a distributed energy management framework[8] under a range of scenarios for spatial planning and ATES operation, using a case study for the city of Utrecht, in The Netherlands.

The following section will frame the contributions of this paper in the context of key challenges for the development of ATES technology. This is followed by a description of the case study and simulation results. The last section of the paper builds on these results to outline policy recommendations, as well as directions for future work.

Background

Technical characteristics of ATES

Shallow geothermal systems are currently the fastest-growing application of geothermal energy[9]. These systems rely on the subsurface to extract or store thermal energy at depths of less than 500m. Aquifer Thermal Energy Storage (ATES) is an increasingly popular form of shallow geothermal energy; ATES systems can be used to reduce building energy demand in temperate climates, by directly pumping groundwater for seasonal energy storage. As such, these systems typically involve at least one pair of coupled wells, which simultaneously infiltrate and extract groundwater from different locations. In winter conditions, extracted groundwater is circulated through a heat exchanger to provide heating in combination with a heat pump. This process reduces the temperature of the extracted water, which is then re-injected into the opposite well at a temperature of 5-10°C. Under summer conditions, this process is reversed: the cooler water which was injected during the winter is extracted, used for cooling, and re-injected at a temperature of 15-20°C. Over time, this leads to the formation of warm and cold zones in the groundwater around each well, which should ideally represent equivalent amounts of thermal energy to maintain the thermal balance of the subsurface. Figure 1 presents the basic principle of the technology.

The development of these thermal zones is a crucial factor for the performance and management of ATES systems: thermal interferences caused by an insufficient distance between warm and cold wells will lead to energy losses, while neighbouring wells of the same type may have a positive mutual thermal influence. However, the monitoring of these thermal zones is technically challenging, and their evolution is tightly linked to local geohydrological conditions – which are themselves difficult to assess. These characteristics yield significant uncertainties in regards to thermal subsurface dynamics, and therefore to the resulting performance of ATES systems.

These uncertainties are compounded by variable weather conditions and building occupancy patterns, which make it difficult to predict building energy demand and maintain a thermal balance in the subsurface. Actual pumping rates are therefore likely to differ from the expected values which are used for system design and planning; inventories of operational systems also indicate significant year-to-year imbalances between heating and cooling[10,11]. Persistent imbalances may compromise the long-term viability of ATES development, by changing temperature distributions in the aquifer and potentially affecting the thermal efficiency of systems[12]. Furthermore, imbalances in the thermally-influenced zones around ATES wells are likely to persist over decades or even centuries, due to the low levels of thermal dissipation in the subsurface.

Management and planning of ATES

Thermal balance and interferences are therefore key elements to consider for the sustainable development of shallow geothermal energy. In response to these issues, management methods for ATES technology have typically followed the precautionary principle[13]. In the Netherlands, revised policies were implemented in July 2013 to reflect new research on the environmental risks of ATES technology; these new policies require permits from provincial authorities for the construction of new ATES systems, which are granted for a given pumping volume on a "first come, first served" basis. Furthermore, design guidelines specify minimal distances between neighbouring wells in order to avoid thermal interactions. These guidelines are based on the average thermal radius R_{th} of the storage wells, i.e. the radius around the wells in which the subsurface temperature is significantly affected; current guidelines specify a conservative distance of $3R_{th}$.

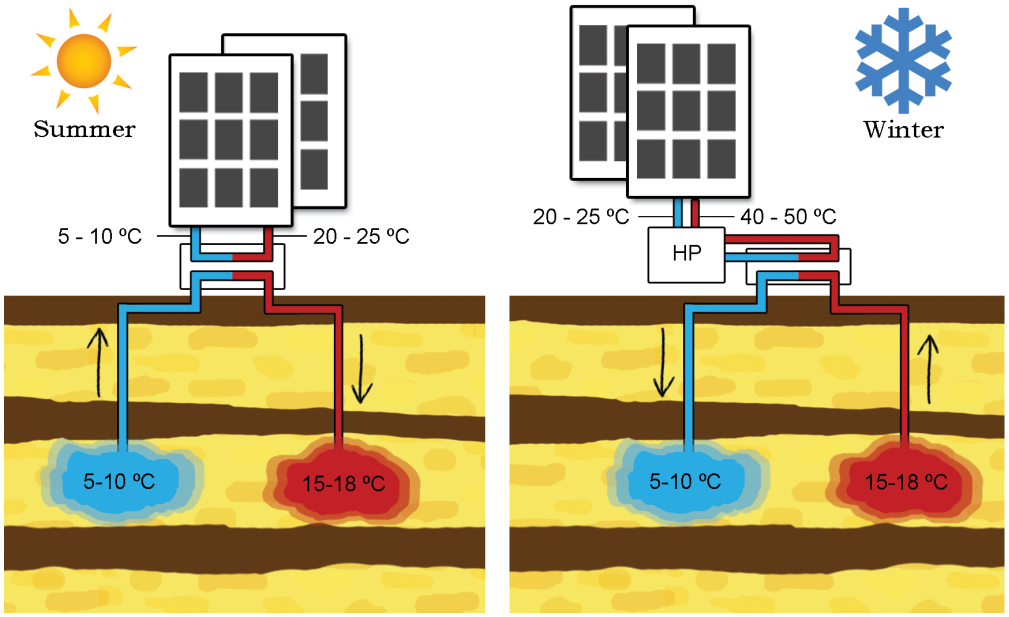

Figure 1. Working principle of Aquifer Thermal Energy Storage

However, these policies take a static, ex ante view of ATES governance, and do not account for the uncertainties which are inherent to ATES adoption and operation. For instance, permits typically do not incorporate feedbacks from operational performance, which could account for systems being used less than expected; an inventory of 125 ATES systems indicated that less than half the permitted storage capacity was typically used[10]. This gives system operators more flexibility to respond to changes in energy demand or operating conditions, but contributes to the present scarcity of space for further development – as allocated space remains unused.

As an alternative, earlier work[14] summarily evaluated the potential of a self-organized approach for ATES management, which could respond more efficiently to changes in short-term operating conditions, as well as longer-term patterns for the adoption of the technology. Empirical evidence indicates that self-organization -– in which cooperative institutional arrangements replace hierarchical planning — may offer an effective alternative for the management of common-pool resources (CPRs)[15]. Considering that the thermal storage potential of the subsurface presents several key features of CPRs[16], self-organization could be appropriate for ATES development due to a relatively small spatial scale, slow resource dynamics, and the high economic benefits of efficient ATES operation[14].

The design of corrective feedbacks and compensation mechanisms will be crucial to preserve the sustainability of the subsurface under such a self-organized approach. This work presents distributed control as a key building block towards a self-organized management regime for ATES; distributed control could support the eventual development of feedback and compensation mechanisms, by providing a framework for the automated exchange of information between ATES users. The case study will test this control approach by first simulating the decoupled, “business-as-usual" operation of ATES systems (hereafter DS), in which individual buildings aim to match the demand and production of thermal energy in the building, while minimizing their operation costs. This is then compared with a distributed multi-agent approach (hereafter DSMPC), which includes information exchange between neighboring buildings to coordinate the operation of their ATES systems, and avoid thermal interferences in the aquifer.

Case study

ATES performance assessment

The simulation case study uses key performance indicators which build on an earlier assessment framework[6], to evaluate the performance of the DS and DSMPC control methods from the perspectives of ATES system owners and policymakers. For the former, three indicators will be used (with details for the computation of each indicator being presented in appendix):

- The average thermal efficiency of ATES systems (η_{tot}), i.e. the fraction of injected thermal energy which is recovered

from the subsurface over a given number of storage cycles;

- The average effective coefficient of performance (COP) of ATES systems, i.e. the ratio between the energy delivered from ATES systems to buildings over a given number of storage cycles, and the energy used to operate the ATES systems;
- The average economic efficiency of ATES systems (νC), defined as specific energy cost savings per unit of water pumped by ATES, relative to a conventional building system delivering the same quantity of heating and cooling energy.

Three additional indicators will be used from the perspective of policymakers:

- The total GHG savings (Δ_{GHG}) obtained by ATES systems, relative to conventional building energy systems which would deliver equivalent heating and cooling energy;
- The average subsurface usage efficiency of ATES systems (ν_{GHG}), defined as the specific GHG savings obtained per unit of subsurface volume which is allocated for thermal storage;
- The average equivalent GHG abatement cost corresponding to ATES use (α_{GHG}), defined as the ratio between ATES operating costs compared to equivalent conventional building systems, and total GHG savings.

These indicators are computed using the parameters summarized in Table 1, and average over two annual storage cycles.

Parameter	Value or range	Unit	Symbol
ATES nominal temperature difference	6	[K]	ΔT
ATES pump efficiency	0.3	[-]	η_p
Boiler efficiency	0.9	[-]	COP_b
Chiller coefficient of performance	3	[-]	COP_c
Heat pump coefficient of performance	4	[-]	COP_{hp}
Grid emission factor for electricity	0.157	$[tCO_2/GJ]$	f_e
Combustion emission factor for natural gas	0.056	$[tCO_2/GJ]$	f_g
Price for electricity	0.05–0.2	$[EUR/kWh]$	C_e
Price for natural gas	0.02–0.1	$[EUR/kWh]$	C_g

Table 1. Parameters used for the assessment of the case studies.

Utrecht case

This simulation case study represents a realistic application for the dynamic management of thermal interactions between ATES systems, by *i)* testing a DSMPC control formulation which can be scaled to manage ATES thermal interactions across multiple buildings, and *ii)* by simulating existing ATES systems and geohydrological conditions in the city center of Utrecht, in the Netherlands. For this case, the building/control models are configured to represent operational uncertainties through a variable demand for ATES storage; further details for the parameterization of the models are supplied in the Methods section. The effective maximum storage capacity of ATES systems is here set by applying a multiplier Q to the nominal permitted storage capacity, with $0.6 \leq Q \leq 1.1$ to match typical operational conditions[10].

Three spatial planning scenarios are used to compare different pathways for the future development of ATES in the area. Following an earlier case study[17], these scenarios assume that ATES wells are built on 9 building plots on which ATES is currently used in the area, starting from a set of 82 currently active or planned wells.

Scenario 1 represents future development under current layout guidelines in the Netherlands (i.e. well distances of 3.0 R_{th}). Scenarios 2 and 3 then simulate revised, denser layout guidelines of 2.5 R_{th} and 2.25 R_{th}, respectively. In all scenarios, simulated new wells are located in available development areas, as long as sufficient space is available under the layout guidelines. These scenarios are illustrated in Figure 2. The dashed lines between wells illustrate the “coupling" constraints for the DSMPC formulation, which aim to avoid interferences between neighboring wells. These constraints are in this case applied to wells of opposite types (i.e. warm/cold) with a relative distance below 2.75 R_{th}. This distance approximately represents the maximum distance at which thermal interactions can be expected to be significant[6].

Inset plots show a bivariate Gaussian kernel density estimate for the distribution of nominal well capacities in each scenario (distinguishing between existing or planned wells, and simulated new wells), and for the distribution of the minimum relative distance to any neighboring well. For instance, this indicates that the simulated new wells in all scenarios have capacities below 100,000 m^3/year, as there is already a lack of space to accommodate larger wells on existing building plots. In parallel, the new wells built in Scenario 3 all have minimum distances of approximately 2.25 R_{th} with other wells, while the sparser guidelines in Scenario 1 lead to a broader distribution on this indicator; we can for instance expect that wells which are not within 3.0 R_{th} of other wells would not be significantly affected by the dynamic management of thermal interactions.

Given that the simulated new wells in Scenarios 2 and 3 are located under different layout guidelines than the existing or planned wells, the management of thermal interactions is likely to impact these groups of wells in different ways – potentially leading to a different distribution of benefits across incumbent ATES users and new adopters. The case study will thus use a simple game-theoretical approach, to test the combinations of ATES usage and energy prices under which cooperation (i.e. participation in an information exchange scheme) would be a Pareto-optimal Nash equilibrium. This analysis assumes that the ATES wells are grouped into “incumbent" and “new" systems.

Results

System performance and distributional effects

Figure 3 presents the average system performance indicators for each spatial planning scenario, as a function of the total volume of water pumped by ATES systems. The DS formulation yields a consistent trend, in which performance tends to decrease within each planning scenario (i.e. with an increase in the allowed pumped fraction Q), and across the planning scenarios (i.e. with an increase in well density). In parallel, the total pumped volume of water increases in proportion to the allowed pumped fraction Q, as expected.

The DSMPC formulation presents significantly different behavior: the total pumped volume of water tends to saturate at $Q = 1.0$, then drops for $Q = 1.1$. This is accompanied by an improvement in the system performance indicators. This behavior is explained by the decrease in usage of wells which are subject to multiple coupling constraints with neighboring wells, and which typically have a lower thermal efficiency due to this density; with an increase in allowed pumped capacity, these “marginal" wells tend to be used less in order to meet the coupling constraints – thus increasing average performance. Figure 11 in appendix details this effect, by plotting the relative usage of the well pairs simulated in Scenario 3, as a function of their decoupled thermal efficiency. Less efficient wells thus tend to be used less when applying the coupling constraints.

For values of $Q = 1.0$, the performance of the systems typically remains at least equal to performance at $Q = 0.6$; Table 3 summarizes these results, computed as “regret" values relative to the DS formulation in Scenario 1 (i.e. $R_{th} = 3.0$).

However, assumptions on energy prices may further complicate the situation; economic performance does not always exactly correlate with thermal efficiency, depending on the relative costs of energy for heating or cooling. As such, whereas high gas prices directly increase cost savings from ATES relative to a conventional boiler, electricity prices have a more complex effect, by affecting the operating cost of ATES well pumps and the building heat pump, as well as cost savings relative to a conventional chiller. Figure 4 presents the relative economic performance of different control/layout combinations, based on the specific energy cost savings per unit of water pumped by ATES in each case . For Scenario 3, this implies that the DSMPC formulation would outperform the DS formulation across all tested energy price combinations, which are based on typical non-household energy prices for electricity and natural gas in the European Union[18,19]). However, energy price combinations which tend to make ATES more relatively profitable overall (i.e. high gas prices and low electricity prices) would slightly penalize the relative performance of the DSMPC/Scenario 3 combination, compared to “business-as-usual” development (DS, Scenario 1). Notably, in conditions where ATES would be less profitable overall, the DSMPC formulation retains a relative advantage due to more efficient pumping schedules.

The analysis has so far considered average results over the full set of active wells. However, Scenarios 2 and 3 in particular may lead to different benefits for existing (or “incumbent") wells, and simulated wells created under different layout guidelines. In this situation, new and incumbent wells may decide to partially cooperate, i.e. to exchange information across their subset of wells only. To evaluate the conditions under which these two groups of users could be assumed to have an incentive to cooperate in exchanging information, Figures 5 and 6 present the effect of different plausible combinations of energy prices and Q values, on the average cost savings of each group of users for Scenario 3. The markers present four possible courses of action: *full cooperation* (i.e. the DSMPC formulation), *only incumbent wells coupled*, *only new wells coupled*, and *no cooperation* (i.e. the DS formulation). The energy cost savings for each action are then considered as payoffs in a 2-player game; shaded subplots indicate that full cooperation is not a Nash equilibrium in a given combination.

Figure 5 thus indicates that relatively high electricity prices may prevent cooperation from being a Nash equilibrium, when combined with a lower ATES usage ($Q = 0.7$) and low gas prices; this combination makes ATES relatively less economically attractive. In this situation, incumbent wells would benefit from full cooperation, while the Pareto-optimal decision for new wells would be to only partially cooperate within their own subset.

However, for $Q \geq 1.0$, the greater overall cost savings from a larger usage of ATES then yield a cooperative Nash equilibrium in all of the energy price combinations, as illustrated in Figure 6.

Collective performance

Given that GHG savings are largely driven by the total pumped volume, a similar pattern holds for the GHG indicators shown in Figure 7 as for system performance. As such, in the DS formulation, the value of both indicators increases monotonically with the allowed pumped fraction Q, but reaches a maximum at $Q = 1.0$ for the DSMPC case.

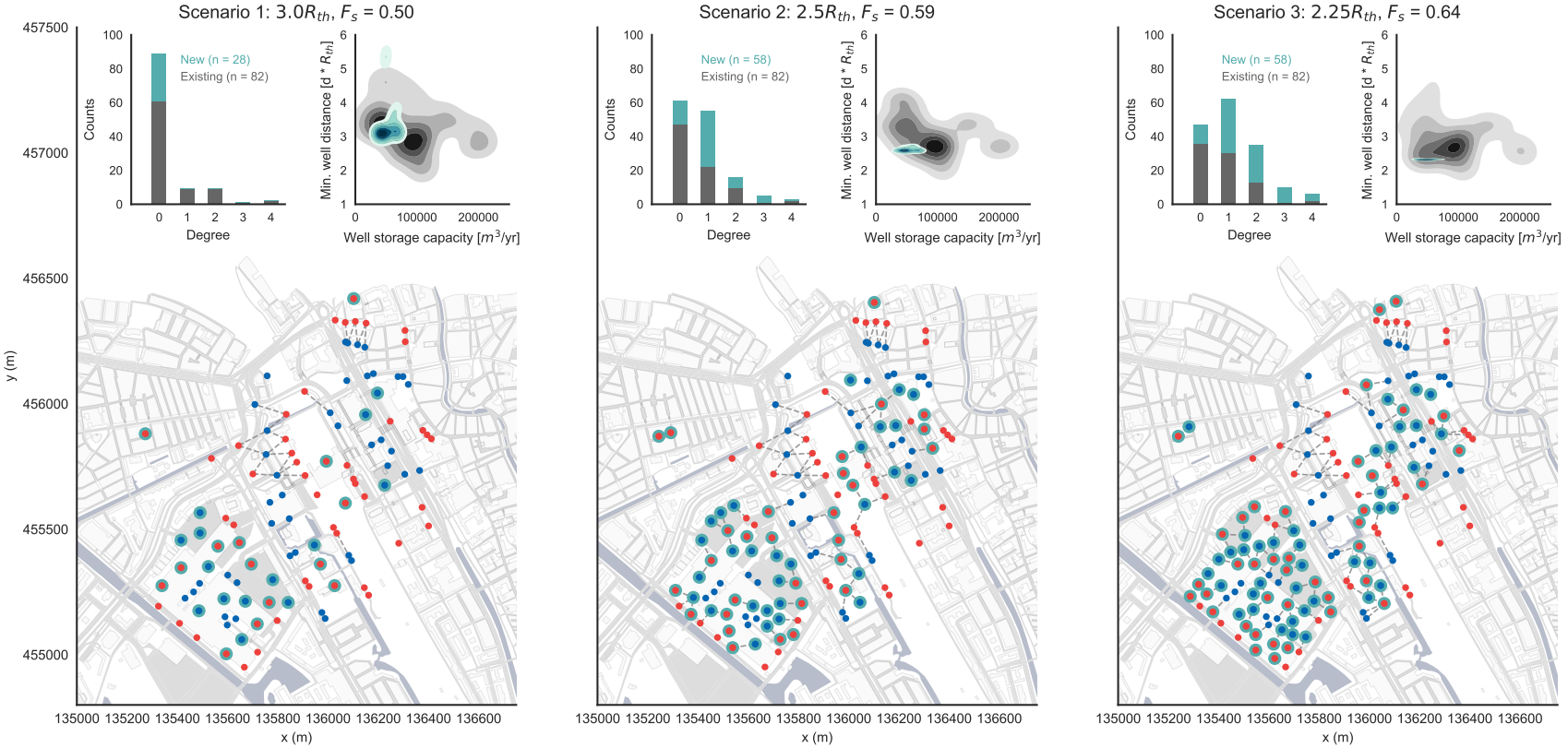

Figure 2. Spatial planning scenarios for Utrecht case study. Dashed lines indicate constrained well pairs; outlined markers indicate existing or planned ATES wells.

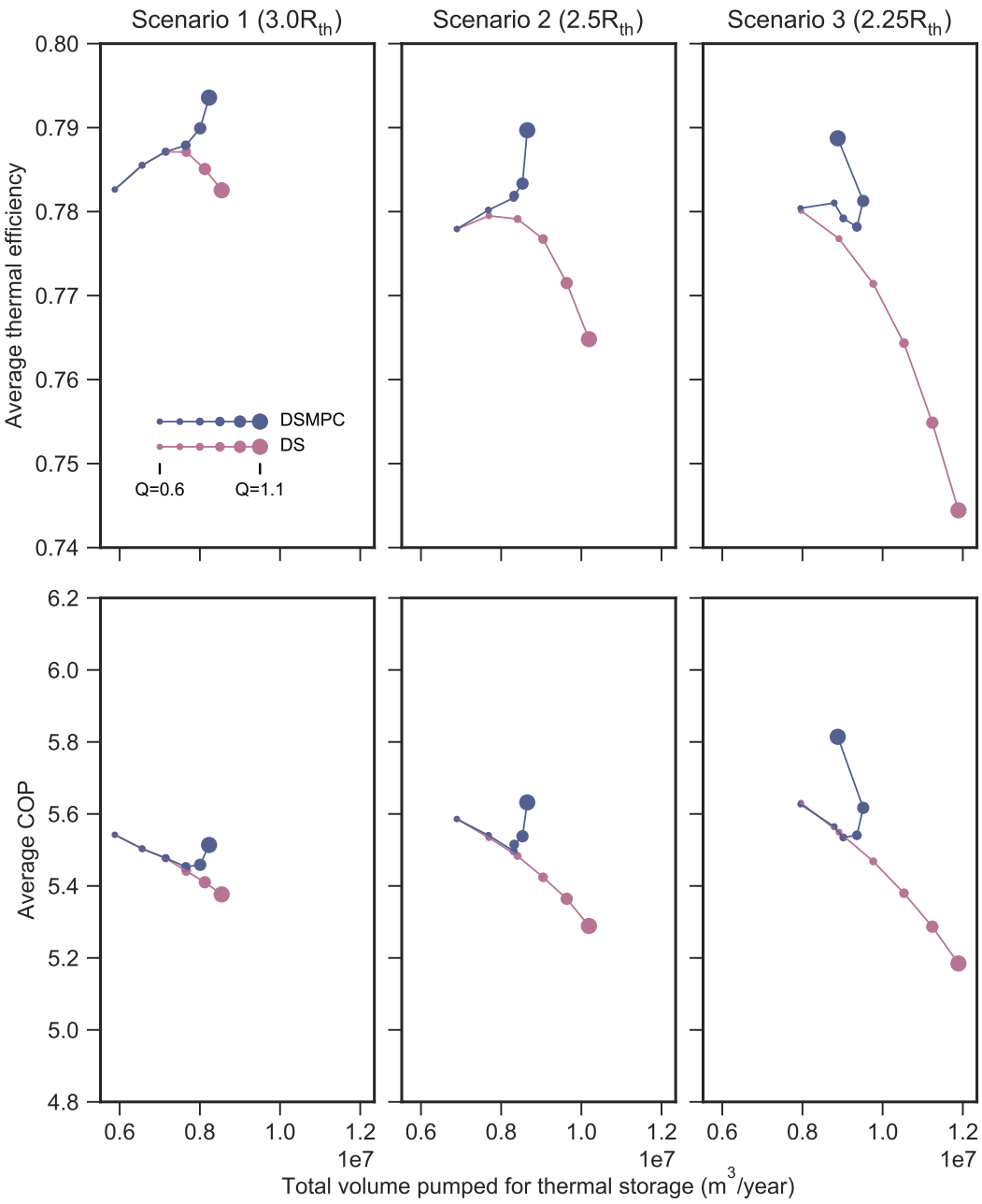

Figure 3. ATES performance indicators for Utrecht case, for each spatial planning scenario: average thermal efficiency (top panel) and coefficient of performance (bottom panel).

As indicated in the tabular results shown in appendix, the increase in specific GHG savings is significant for denser layout guidelines (e.g. 37% with the DSMPC formulation in Scenario 3). The highest specific GHG savings are obtained with the DS formulation in Scenario 3, which maximizes the total pumped water volume; however, the associated decrease in system performance would likely be unacceptable for ATES owners.

This trade-off can be expressed through the equivalent marginal GHG abatement cost, which relates energy cost savings and GHG savings. The left panel of Figure 8 presents the GHG abatement cost for the DSMPC formulation in Scenario 3; the negative values indicate that the additional development of ATES systems allowed in this case would nonetheless be economically attractive compared to conventional energy. In parallel, the right panel presents the marginal GHG abatement cost which is obtained by comparing the DSMPC formulation in Scenario 3, with the "business-as-usual" case (DS, Scenario 1). As

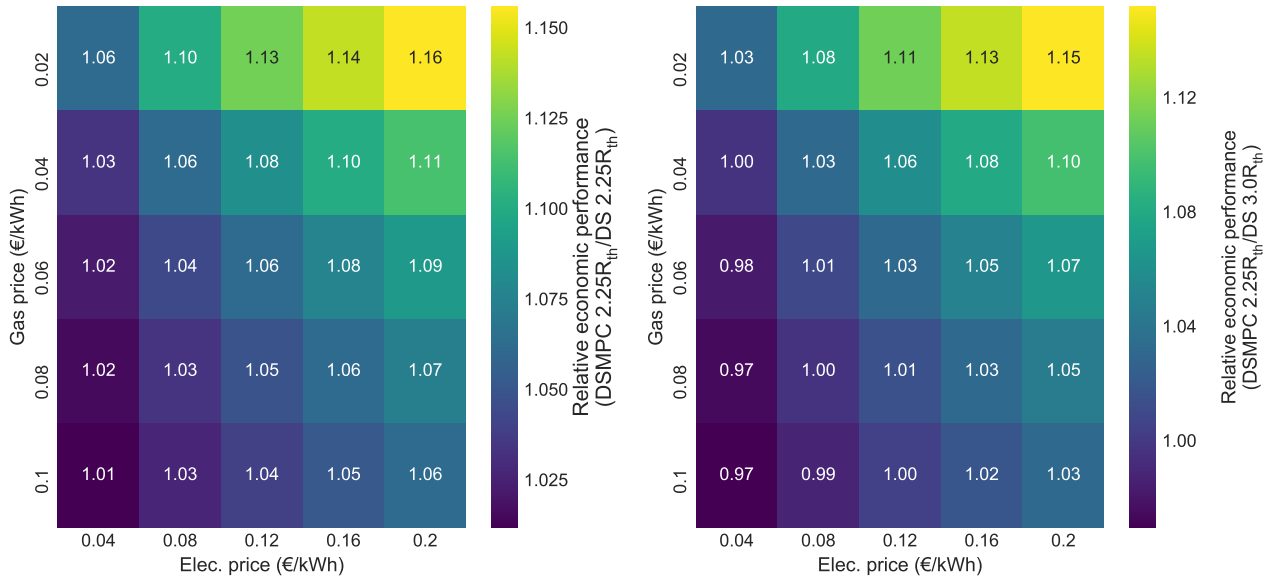

Figure 4. Relative economic performance across different control/layout combinations. Left panel: DSMPC compared to DS, for Scenario 3 ($2.25R_{th}$). Right panel: DSMPC for Scenario 3, compared to DS for Scenario 1.

previously shown in Figure 4, a higher gas price combined with a relatively lower electricity price tends to make the DSMPC approach relatively less economically attractive. However, considering the overall improvements in GHG savings which would be supported by this approach, the equivalent GHG abatement cost is relatively low; this cost is for instance below typical carbon prices for the European Union Emissions Trading System for the 2017-2018 period.

Under the assumptions used to parameterize the models, this implies that denser ATES development with a DSMPC approach would remain an economically attractive GHG abatement option for policymakers, even under an unfavorable combination of energy prices. Furthermore, the opposite combination of energy prices (i.e. low gas price and high electricity price, which tends to make ATES more economically sensitive to pumping schedules) would favor the DSMPC approach, yielding negative marginal abatement costs.

Conclusions

Current methods for the planning and operation of ATES systems lead to an inefficient trade-off between private and public interests, by limiting the deployment of the technology – and thus energy savings – in the dense urban areas which account for a growing portion of energy use in the built environment. This situation is motivated by the risk of a “tragedy of the commons" which could be caused by uncontrolled thermal interferences between ATES systems sharing an aquifer. As a starting point towards an improved management regime which could resolve this trade-off, this work assessed an approach based on the distributed control of ATES systems, in which information exchange would support the dynamic management of thermal interactions between neighboring ATES systems. Based on the results of a simulation case study for the city center of Utrecht, in The Netherlands, this approach could significantly improve greenhouse gas savings from ATES, without compromising the performance of individual systems. Compared to a “business-as-usual” case, information exchange – combined with a denser layout policy for ATES wells – respectively yielded improvements of 21% and 38% in total GHG savings and specific GHG savings per unit of allocated subsurface volume, at a comparable average level of economic performance.

A coordinated approach to ATES operation could thus change the structure of the trade-off between private and public interests: under plausible operating conditions, the exchange of information across ATES systems could lead to a “win-win” situation for policymakers and operators, by increasing collective GHG savings without penalizing economic performance. However, this approach would lead to a different compromise, under which ATES operators would trade off the implicit value of information about their use of ATES and other building energy systems. The privacy implications of smart energy systems have drawn increased scrutiny in the literature[20–22]; in the case of industrial energy users, thermal demand profiles could for instance be used to infer sensitive information about production processes[23]. Similarly, in the case of residential users, aggregation across multiple sources and levels of energy usage may make it impossible for participating individuals to offer genuinely informed consent towards the use of their data[21]. Although dedicated research is needed to assess these issues in the specific

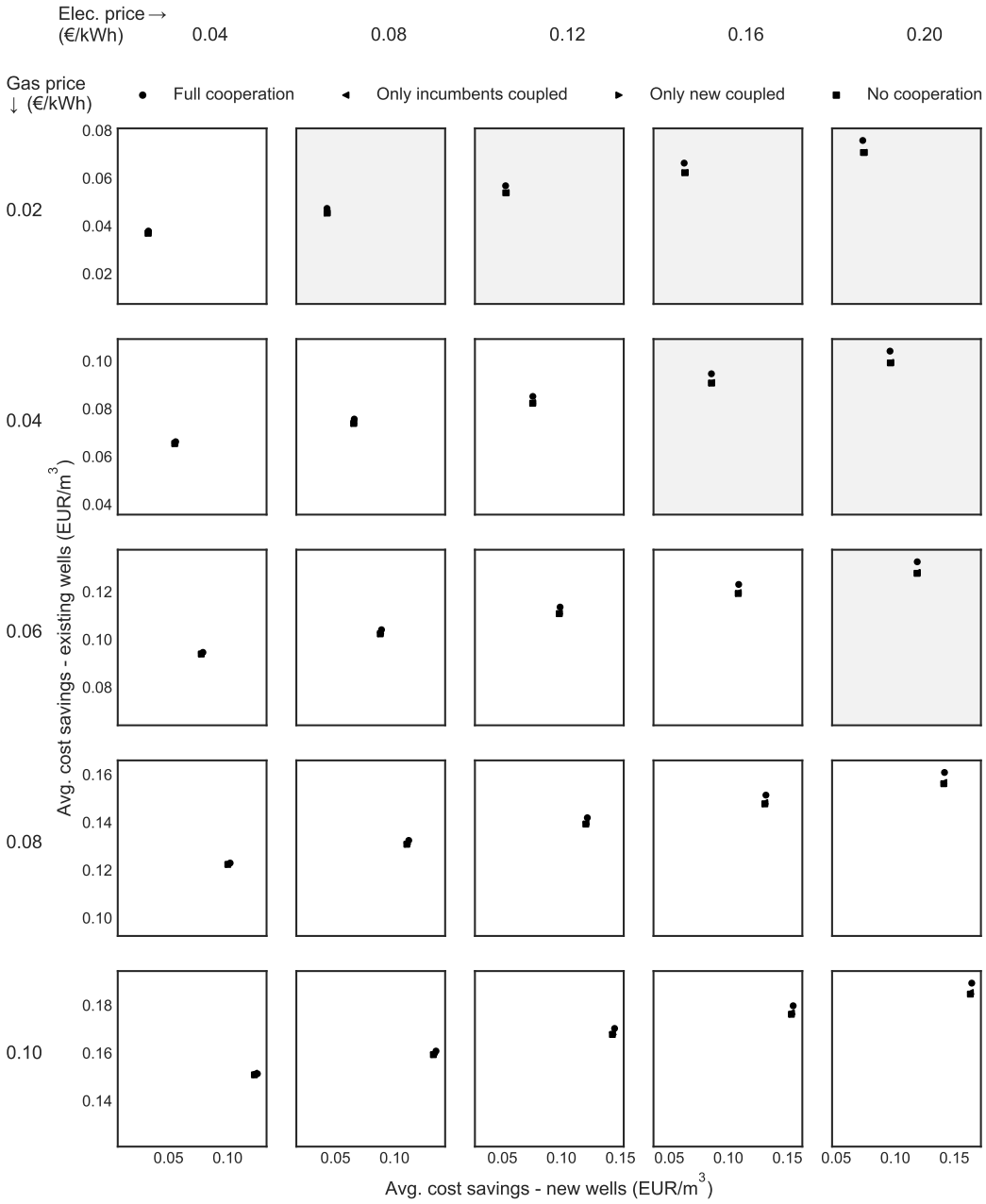

Figure 5. Game-theoretical analysis for cooperation between incumbent and new wells, as a function of gas and electricity prices, for $Q = 0.7$ and Scenario 3. Shaded subplots indicate that full cooperation is not a Nash equilibrium in a given combination of energy prices.

context of ATES, we note that the DSMPC approach is entirely compatible with differential privacy methods, under which the required information is pre-processed to maintain a level of privacy for the participating agents[24]. This would then entail a trade-off between the bandwidth of exchanged information, and its reliability towards the management of thermal interactions.

Finally, we emphasize that taking advantage of the dynamic management of thermal interactions will also require revised spatial planning policies: the current guidelines used to plan ATES systems in the Netherlands are effective at avoiding thermal interactions between systems, which implies there would be little benefit in their management. This was supported by the results of the simulated case study, in which a coordinated approach showed limited gains under current ATES well layout guidelines of $3.0R_{th}$. We note that the dynamic management of thermal interactions would offer greater benefits in relatively shallower aquifers, in which seasonal pumping patterns yield larger variations in the thermal radii of storage wells; due to the

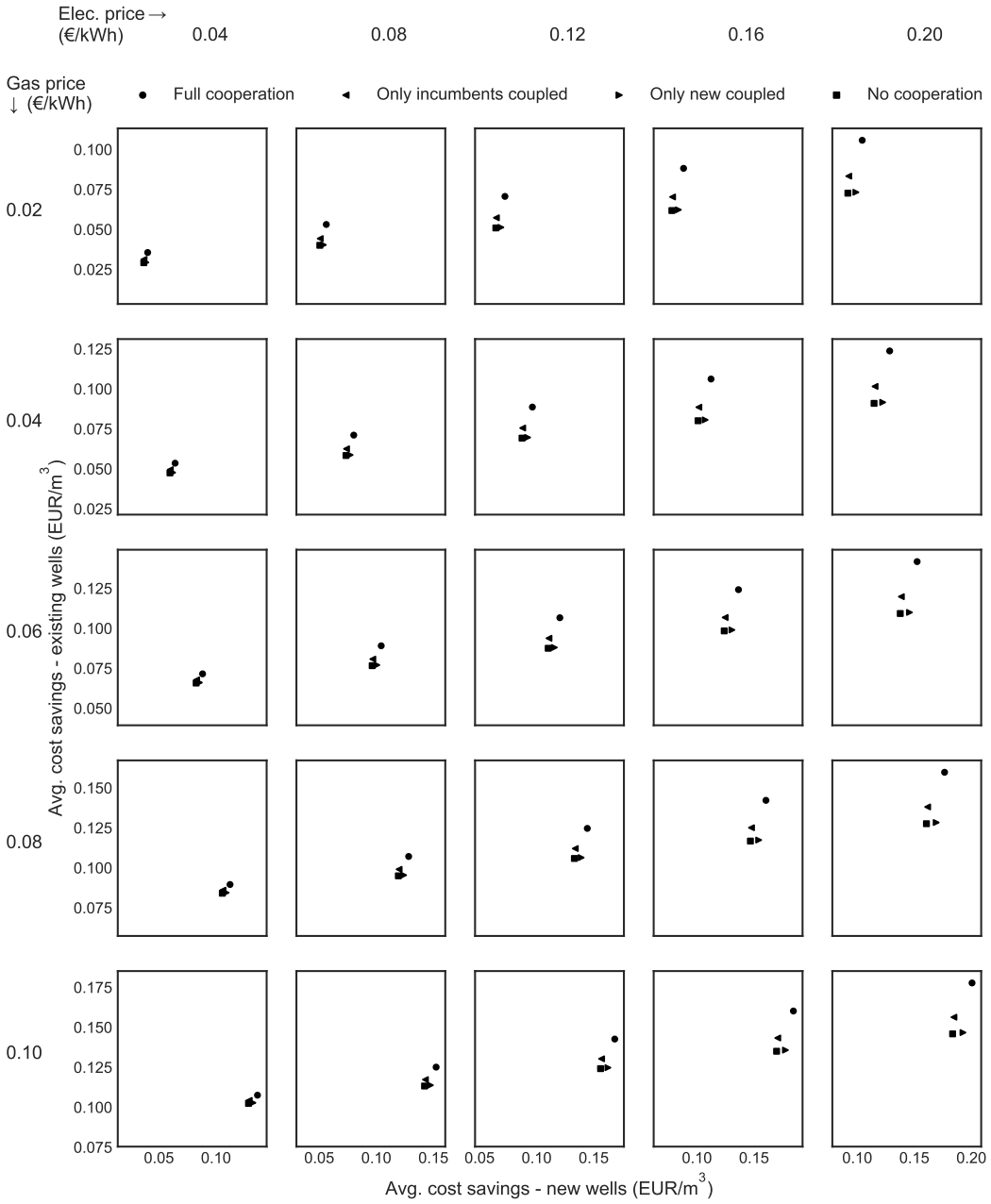

Figure 6. Game-theoretical analysis for cooperation between incumbent and new wells, as a function of gas and electricity prices, for $Q = 1.1$ and Scenario 3.

relatively larger storage footprint of wells in the horizontal plane, shallower aquifers are more likely to experience a scarcity of space for new ATES systems, making the management of interactions particularly relevant in these cases. Crucially, the current rapid deployment of ATES provides a window of opportunity to apply such improved methods for the planning and operation of systems, as policymakers and ATES operators may otherwise become locked into suboptimal practices.

Methods

Model predictive control for ATES systems

Model predictive control (MPC) is a widely used modern optimal control strategy, which typically offers an attractive trade-off between optimality and computational cost. The concept of MPC is simple: predict the behaviour of a system given its model

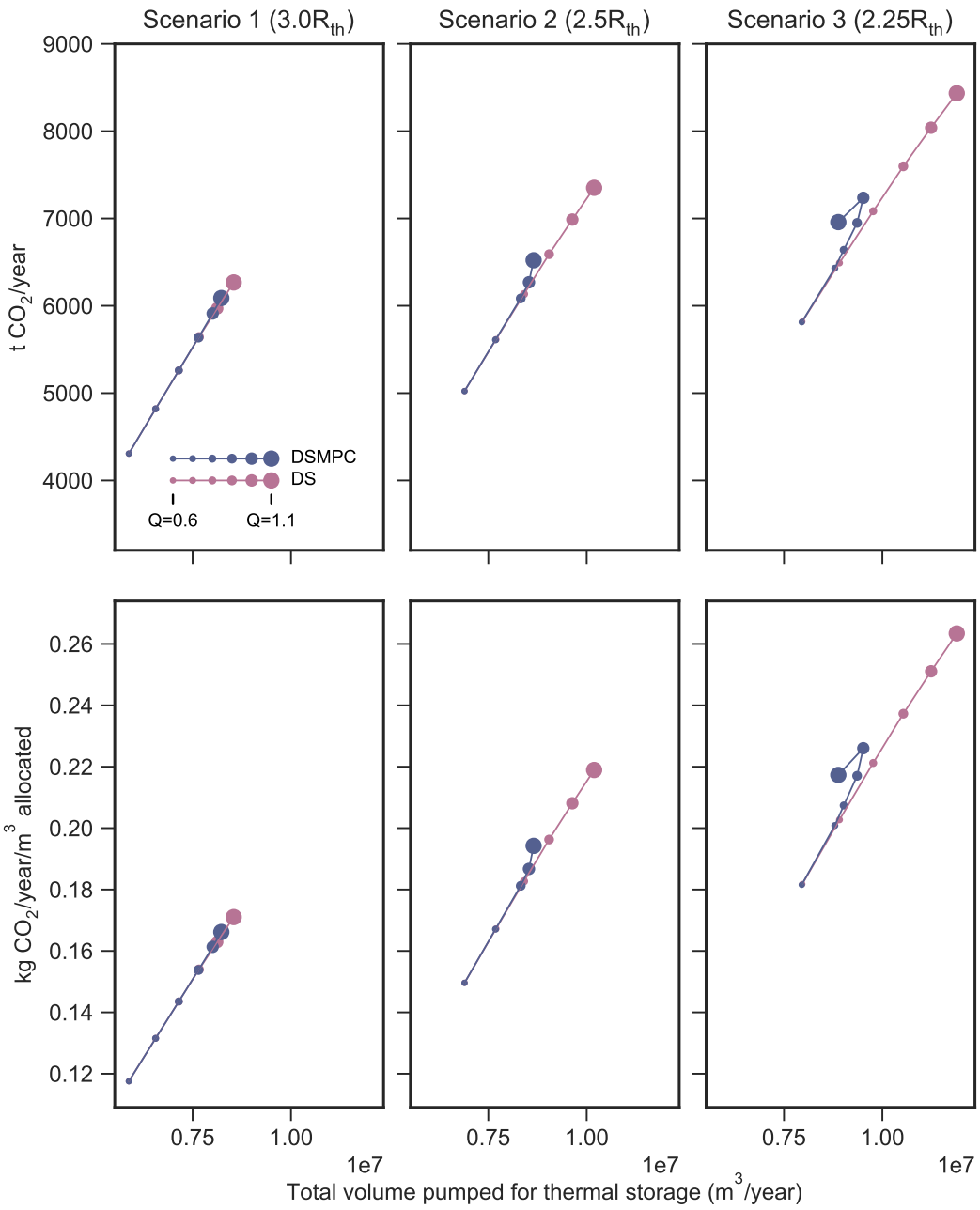

Figure 7. Collective performance indicators for Utrecht case, for each spatial planning scenario: total annual GHG savings (top panels); specific annual GHG savings per allocated unit of subsurface volume (bottom panels).

and measurements of the current state of the system, and given a hypothetical control input trajectory or feedback control policy. The control inputs are parametrized by a finite number of variables which denote a finite number of degrees of freedom. The predicted cost of the problem is optimized over these variables, using a given cost function. The control input is then applied to the system in a receding horizon fashion, wherein only the first element of the predicted control input sequence is applied to the system at the current time instant. The horizon is shifted at the next time instant, and the optimization problem is carried out again to obtain a new sequence of control inputs.

The receding horizon strategy is instrumental in reducing the gap between the predicted response and the actual response of the system; this strategy also provides a certain amount of robustness to uncertainty that can arise in the system. This uncertainty arises in the form of uncertain model parameters – which is known as multiplicative model uncertainty – and in the form of

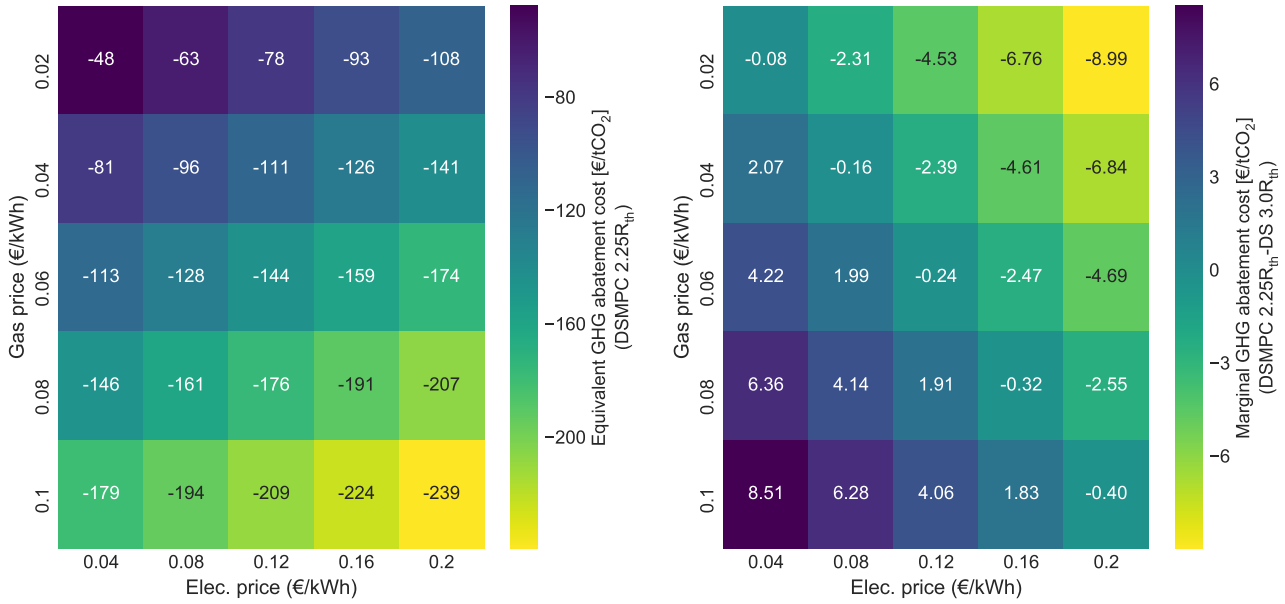

Figure 8. Left panel: equivalent GHG abatement cost for DSMPC in Scenario 3 ($2.25R_{th}$). Right panel: marginal GHG abatement cost for DSMPC in Scenario 3, compared to "business-as-usual" development (DS, Scenario 1).

additive disturbances appearing from external sources, which is known as additive uncertainty. MPC has the ability to handle operations of processes within well-defined operating constraints, which is not always a given with other methods, but which allows e.g. equipment limits to be represented realistically. These constraints are handled systematically during the design and the implementation of the controller. MPC can respond to structural changes such as actuator and sensor failures, or changes in system parameters, by adapting the control strategy at every time step of execution of the algorithm. For these reasons, MPC has evolved from a basic multivariable process control technology, to a technology that has become widely accepted in industry – which includes the operation of building energy systems or smart thermal grids[25–28]. Compared to conventional methods such as PID controllers, the ability of MPC to handle large-scale dynamical systems under strict constraints offers several advantages for these applications.

Centralized control

[29] presented a MPC formulation for a building climate comfort (BCC) system combining ATES with conventional heating/-cooling equipment (i.e. a boiler and chiller). This formulation was first expressed as a finite-horizon, mixed-integer quadratic optimization problem for a single building; as such, this single-agent formulation aims to match the demand and production of thermal energy in the building, while minimizing operation costs and satisfying physical constraints for heating and cooling capacity. This problem was then extended to a centralized multi-agent formulation for multiple buildings. This maintains the individual optimization problems for each building and adds coupling constraints between neighbouring buildings, in order to avoid mutual interactions between ATES systems. These formulations build on a robust randomized approach to remain computationally tractable while meeting a desired level of reliability in regards to the constraints.

The coupling constraints rely on the single-agent state variables of the individual ATES systems, which are modelled using first-order difference equations to represent the water volume and thermal energy stored by each building. These equations assume that each ATES system is composed of one warm well and one cold well, which are physically linked; the control variable for the pump flow rate in heating and cooling modes (H and C) is given by $u^H_{a,k}$ and $u^C_{a,k}$ $[m^3h^{-1}]$ respectively, for each sampling time $k = 1, 2, \ldots$. Taking $\tau[h]$ as the sampling period, the usable volume of water stored in the warm and cold ATES wells, V^H_a and V^C_a, is then given by:

$$\begin{aligned} V^H_{a,k+1}[m^3] &= V^H_{a,k} - \tau(u^H_{a,k} - u^C_{a,k}) \\ V^C_{a,k+1}[m^3] &= V^C_{a,k} - \tau(u^H_{a,k} - u^C_{a,k}) \end{aligned} \tag{1}$$

Assuming the stored volumes can be approximated by a cylinder with a height equal to the well screen length $L[m]$, and taking a constant aquifer porosity n, this yields hydraulic radii r^H_h, r^C_h for the warm and cold wells:

$$r^H_{h,k}[m] = \sqrt{\frac{V^H_{a,k}}{n\pi L}}$$
$$r^C_{h,k}[m] = \sqrt{\frac{V^C_{a,k}}{n\pi L}} \tag{2}$$

The equivalent thermal radii r^H_{th} and r^C_{th} of the warm and cold wells are then given by:

$$r^H_{th,k}[m] = \sqrt{\frac{c_w V^H_{a,k}}{c_{aq}\pi L}}$$
$$r^C_{th,k}[m] = \sqrt{\frac{c_w V^C_{a,k}}{c_{aq}\pi L}} \tag{3}$$

where c_w and c_{aq} are the specific heat capacity for water and for the aquifer, respectively. For each building agent i, constraints can then be added to the optimization problem in order to avoid overlap between neighboring well radii, so that:

$$(r^H_{th,k})_i + (r^C_{th,k})_j \leq \theta d_{i,j}, \quad j \in \mathcal{N}_i \tag{4}$$

where $\mathcal{N}_i$ is the set of neighboring agents of agent i, $d_{i,j}[m]$ is a given distance between wells for agents i and j, and θ is a constant which can be used to adjust the influence of the constraint (so that a larger value will tend to relax the coupling constraint). The coupling constraint can equivalently be applied to hydraulic radii by choosing a different θ parameter.

These decoupled and centralized multi-agent formulations (i.e. without and with ATES coupling constraints; DS and CS) are used for the idealized 3-building ATES simulation study presented in supplementary material, with an hourly sampling time and a day-ahead prediction horizon.

Distributed control

In practice, the centralized formulation can become computationally too costly to solve for a larger number of agents; in these conditions, distributed control offers improved performance. Distributed MPC aims to replace large-scale centralized optimization problems with several smaller-scale problems, which can be solved in parallel. These problems make use of partial information from other subsystems to implement a distributed solution. In the presence of uncertainties, however, the main challenge in formulating a distributed MPC is the design of a suitable communication scheme to exchange this information between subsystems.[8] provide an appropriate technique to decompose a large-scale scenario-based MPC problem into distributed problems, which exchange a certain number of samples with each other to compute local decisions.

This approach implements the same ATES well coupling constraints as the centralized formulation, using a hierarchical scheme;[8] showed this formulation to be practically equivalent to the CS coupling formulation. An upper control layer thus applies the coupling constraints to coordinate the operation of neighboring ATES systems, with weekly time steps and a 3-month prediction horizon. A lower layer then implements the same individual control problem for each building as in[29]. This method can be applied efficiently for larger sets of agents, with computational runtimes scaling $\mathcal{O}(n)$ in proportion to the number of agents. This formulation (DSMPC) is therefore used for the large-scale ATES simulation study.

Coupled building/geohydrological simulation

This work relies on a coupled simulation architecture which links a building/control model in MATLAB, an agent-based model of ATES planning in NetLogo[30], and a geohydrological model of groundwater dynamics in MODFLOW/SEAWAT[31,32]. The three model components are linked through an object-oriented Python architecture, so that Python objects form the interface between the three models. Figure 9 illustrates the basic architecture and shows the data exchanges, which are facilitated by the FloPy pre/post-processor for MODFLOW/SEAWAT[33].

The NetLogo agent-based model is used to locate new simulated ATES wells in a 2000m x 2500m grid, on which GIS data is overlaid to generate exclusion areas corresponding to roads, buildings, and waterways. The storage capacity of each ATES system was randomly picked from a distribution describing the occurrence of ATES systems in the Netherlands contained in a dataset of the permitted capacity of over 430 ATES systems in the Netherlands, as described in[6].

The control formulations for the decoupled, centralized and distributed cases are implemented in MATLAB 2016a, using the YALMIP interface[34] with the Gurobi 8.0 solver. The controllers are simulated using given energy demand time series for

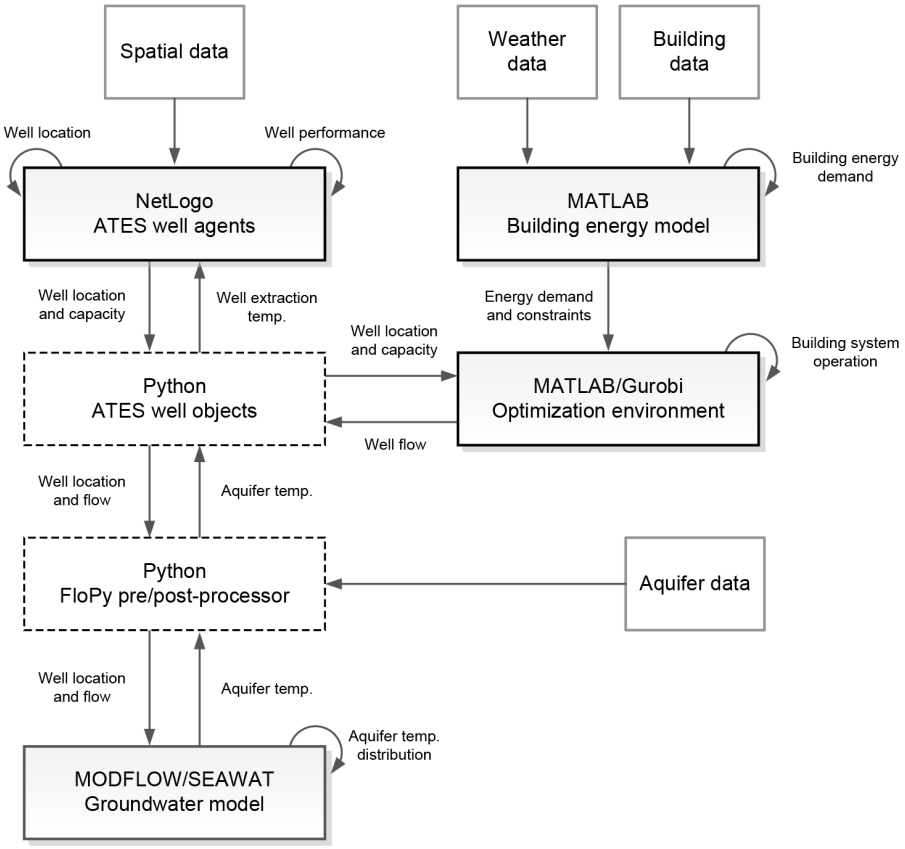

Figure 9. Simulation architecture

the building agents, which are generated by a stochastic version of the Low Energy Architecture (LEA) simulation model (detailed in[35–37]). This energy balance model accounts for weather conditions, building characteristics, and occupancy patterns, and generates the heating and/or cooling demand profiles which are required to maintain a desired indoor temperature. In this application, time series for energy demand, and the corresponding control action for ATES pumping rates of each agent, are computed *ex ante* at an hourly resolution. The ATES pumping rates are then aggregated at a weekly scale and simulated as equivalent ATES well flows in the MODFLOW/SEAWAT groundwater model.

Aquifer properties

The Utrecht case study presents two key differences from the idealized aquifer model which is presented in supplementary material: ambient groundwater flow in the area (approximately 10 m/y) may influence recovery performance through advection losses, while the greater thickness of the aquifer reduces the "footprint" of the wells in the horizontal plane and its variation over storage cycles, so that the effect of well couplings may be less apparent.

The case study relies on a 3000m x 3000m cutout of the Hydromedah groundwater model for the Utrecht region[38,39]; this model had previously been adapted to include ATES wells, as detailed in[17]. As such, the grid is rediscretized in the horizontal plane to refine cells around the ATES wells in each spatial planning scenario, with a grid size varying from 8m at the center of the wells, to 16m at the border of the model; the corresponding arrays for horizontal conductivity and groundwater head are rediscretized using bilinear interpolation. The ATES wells are located in a confined layer with an average thickness of 26m. In addition, the standard MT3DMS packages are parameterized using the same assumptions as the idealized aquifer model, in order to include relevant transport processes.

Climate properties

Changes in the energy demand of buildings over time are a key component of operational uncertainties for ATES. These changes may be caused by daily variations in weather conditions or building occupancy, but also by longer-term trends in climate which may eventually affect the balance between heating and cooling demand. To evaluate the performance of the CS formulation under variable building energy demand, a set of representative weather profiles was therefore derived from the four KNMI'14 climate scenarios[40].

These scenarios (G_L, G_H, W_L, W_H) are defined by moderate or high increases in global mean temperature (G and W respectively, with an increase of 1°C and 2°C by 2050), and low or high changes in air circulation patterns (L and H, respectively). The change in temperature under the G and W scenarios is roughly consistent with the standard RCP 4.5 and RCP 8.5 emissions scenarios[41].

In order to simulate building energy demand under these scenarios, a 3-year hourly time series was first obtained for observed air temperature (2011-01-01/2014-01-01) at the De Bilt weather station. In parallel, synthetic daily time series were generated using the KNMI time series transformation tool[42], to simulate air temperature at the same location under each of the climate scenarios. These series were generated for a 3-year period under reference conditions in 2010, and under scenarios for 2050. To simulate energy demand under these synthetic series at an hourly resolution, the observed hourly time series was then modified using a shifting/stretching method[43] to match the long-term trends described by the synthetic series. The method is described by Equation 1, where $\Delta\mathrm{TMAX}_m$, $\Delta\mathrm{TMIN}_m$ and $\Delta\mathrm{T}_m$ are the predicted changes in monthly maximum, minimum and mean temperature, using the synthetic series for 2050 relative to 2010. $(t_{0max})_m$ and $(t_{0min})_m$ are the observed monthly mean daily maximum and minimum temperatures, while t_0 is the observed hourly temperature time series. The scaled hourly temperature series t is then:

$$\begin{aligned} \alpha &= \frac{\Delta\mathrm{TMAX}_m - \Delta\mathrm{TMIN}_m}{(t_{0max})_m - (t_{0min})_m} \\ t &= t_0 + \Delta\mathrm{T}_m + \alpha \cdot (t_0 - (t_0)_m) \end{aligned} \tag{5}$$

Following this method to generate hourly time series for each of the climate scenarios, Figure 10 presents the simulated 3-year temperature time series (left panel; smoothed over a 30-day moving average), and the corresponding average annual thermal imbalance towards heating for building 1 of the idealized case study, over the last two years of the simulated time series (right panel; defined as $(H-C)/(H+C)$, where H and C are the building energy demand for heating and cooling, respectively). This indicates that the climate scenarios shift building energy demand from primarily heating-driven (+10% imbalance under G_L), to cooling-driven (-5% under W_H).

These trends can be compared with typical year-to-year variations in ATES thermal balance which are caused by weather fluctuations.[10] presents results for a sample of 125 Dutch ATES systems over the 2010-2014 period, with the average ATES thermal balance showing a positive relationship with the deviation of heating degree-days from the average. As such, the average annual imbalance varied between -16% and +23%, following variations in degree-days from -29% to +20% of the average. While the magnitude of long-term climate trends may thus remain less significant than annual weather variations for

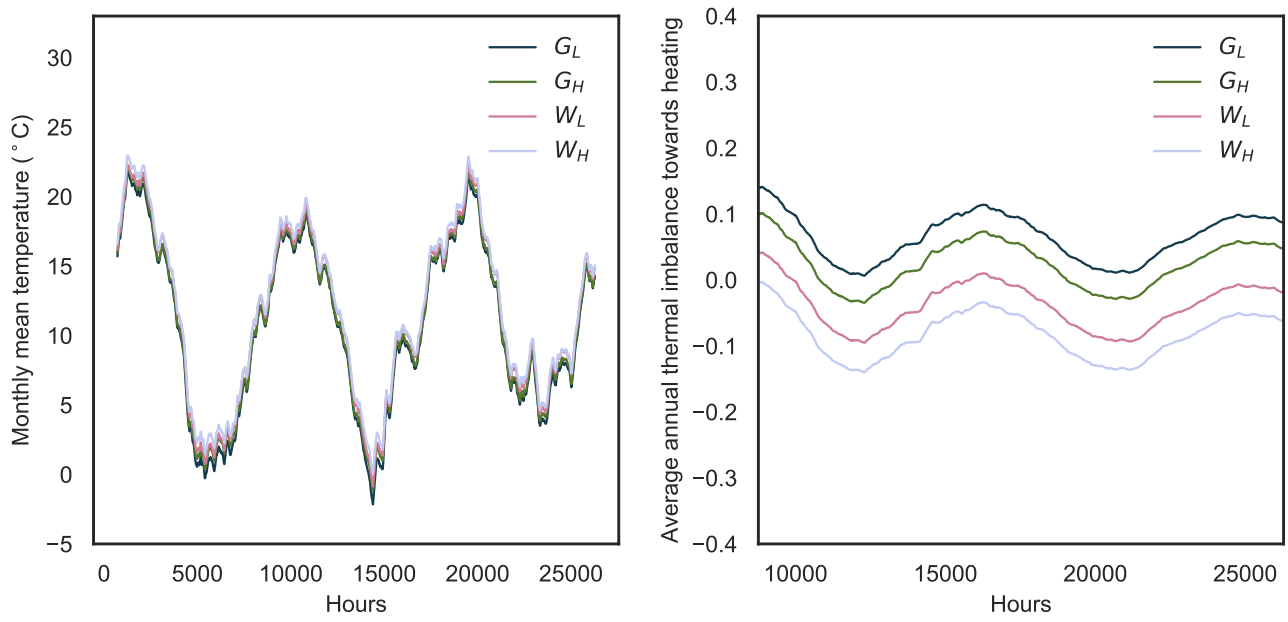

Figure 10. Left panel: Simulated time series for hourly average temperatures under each KNMI climate scenario at the De Bilt weather station, smoothed over a 30-day moving average. Right panel: Simulated annual thermal imbalance towards heating, under each KNMI climate scenario (Building 1 of the idealized case study)

ATES thermal balance by 2050, a consistent trend towards warming would make it more difficult to meet balance requirements. These trends should therefore be acknowledged in the planning and operation of ATES systems.

Assessment framework[1]

Energy use and emissions of ATES systems

The energy balance of the heat pump is used to trace back the heating and cooling demand (E_h, E_c) of the associated buildings and the energy consumption by the heat pump. The total heating capacity for the building provided by the heat pump is described by two basic relations:

$$P_h = P_{ATES} + P_e \quad \& \quad COP_{hp} = \frac{P_h}{P_e} \tag{6}$$

where P_h [W] is the heating capacity deliverable to the building; P_{ATES} [W] the thermal heating power retrieved from the groundwater, P_e [W] the electrical power consumed by the heat pump and COP_{hp} coefficient of performance of the heat pump. Equation 6 shows that all electric power fed to the heat pump contribute to the heat output. When it is assumed that 100% of the heating and cooling demand of the building is delivered by the ATES system, the heating capacity and total heat energy ($E_{h,ATES}$) from the groundwater between times t and t_0 equals

$$E_{h,ATES}(t_0 \rightarrow t) = c_w \int_{t_0}^{t} P_{ATES} dt = c_w \Delta \bar{T}_h \int_{t_0}^{t} Q dt = c_w \Delta \bar{T}_h V_h \tag{7}$$

with

$$P_{ATES} = c_w Q(T_w T_c) = c_w Q \Delta T_h \tag{8}$$

The integration is done for the whole heating season ($t_0 \rightarrow t$). V_h [m^3] is the given seasonal volume of groundwater required for heating. ΔT [K] is the instantaneous temperature difference between the warm (T_w) and cold (T_c) well, is the average

[1] Based on Bloemendal et al.[6]

temperature difference during heating season, Q [m3/h] is the groundwater flow from the warm well to the cold well and c_w [J/m^3/K] is the volumetric heat capacity of the water. With V_h substituted in equations 6 and 8, equation 9 yields the heat E_h [J] delivered to the building over the heating season:

$$E_h = c_w \Delta \bar{T}_h V_h \frac{COP_{hp}}{COP_{hp} - 1} \tag{9}$$

The cooling delivered to the building is calculated using the same equations, while distinguishing between free cooling and heat pump cooling. An absolute temperature threshold of 9°C was set for the cold well above which no free cooling is assumed possible. When the extraction temperature of the cold well surpasses this threshold, the heat pump is used to meet the cooling demand and resulting heat is transferred to the warm well via the condenser of the heat pump. The total cooling delivered to the building then follows from:

$$E_c = c_w \Delta \bar{T}_{c,fc} V_{c,fc} + c_w \Delta \bar{T}_{c,hp} V_{c,hp} \frac{COP_{hp} - 1}{COP_{hp} - 2} \tag{10}$$

in which $V_{c,fc}$ and $V_{c,hp}$ are the groundwater volumes required for free cooling and cooling by the heat pump and $\Delta T_{c,fc}$ and $\Delta T_{c,hp}$ are the average temperature differences between the warm and cold well for free cooling and cooling by the heat pump respectively. Note that the heat pump COP is 1 lower during cooling. The total energy consumption of the ATES system (E_{ATES}) is completed by including the pump energy consumption. Substituting equations 6 into 9 and 10 yields:

$$E_{ATES} = \frac{E_h}{COP_{hp} - 1} + \frac{E_{c,hp}}{COP_{hp} - 2} + \frac{(V_h + V_{c,fc} + V_{c,hp}) \Delta p}{\eta_p} \tag{11}$$

where Δp is the lifting pressure generated by the groundwater pump and η_p its nominal efficiency. The effective coefficient of performance of the ATES systems corresponds to the ratio between the quantities of energy which are delivered and used:

$$COP = \frac{E_h + Ec}{E_{ATES}} \tag{12}$$

In parallel, the energy efficiency (η) of a well over the simulation period is calculated in weekly steps by dividing the extracted amount of thermal energy by the infiltrated amount of thermal energy. The thermal efficiency taken over all the wells in the model (η_{tot}) is the average of the individual efficiencies, weighted by the individual total storage volume of the wells ($V_i = V_{h,i} + V_{c,fc,i} + V_{c,hp,i}$)

$$\eta_{tot} = \frac{\sum_{i=1}^{n} \eta_i V_i}{\sum_{i=1}^{n} V_i} \tag{13}$$

The equivalent GHG emissions [tCO_2] are retrieved by calculating the CO_2 emissions of the considered ATES systems:

$$GHG_{ATES} = \sum_{i=1}^{n} E_{ATES,i} f_e \tag{14}$$

where f_e [tCO_2/GJ] is the grid emission factor for electricity, E_{ATES} [GJ] is the electricity consumption of the ATES system, and n the number of active ATES wells. The calculation assumes a representative emissions factor for delivered electricity in the Netherlands.

Energy use and emissions of reference boiler/chiller systems

As a reference for technical and economic performance of ATES systems, the calculation considers a conventional climate control installation which would deliver the same amount of heating E_h [GJ] and cooling energy E_c [GJ] to the building. It is assumed that natural gas is used for heating in a boiler with combustion efficiency COP_b, and that electricity is used for a cooling machine operating at a constant coefficient of performance COP_c. The energy consumption and greenhouse gas emissions [tCO_2] for these buildings then equal:

$$E_{boiler} = \frac{E_h}{COP_b} \quad \& \quad E_{chiller} = \frac{E_c}{COP_c} \tag{15}$$

$$GHG_{conv} = \sum_{j=1}^{n} (E_{boiler,j} f_g + E_{chiller,j} f_e) \tag{16}$$

in which f_e $[tCO_2/GJ]$ is the emission factor for gas and m the number of active conventional systems (which we here consider to be equal to the number of ATES systems).

Economic parameters

Operational costs for ATES and conventional systems can be computed similarly to GHG emissions, using the electricity price C_e $[EUR/GJ]$ and natural gas price C_g $[EUR/GJ]$ instead of the emission factors:

$$C_{ATES} = \sum_{i=1}^{n} E_{ATES,i} C_e \tag{17}$$

$$C_{conv} = \sum_{j=1}^{n} (E_{boiler,j} C_g + E_{chiller,j} C_e) \tag{18}$$

The economic efficiency of ATES can then be expressed as cost savings per total volume of water used for storage $[EUR/m^3]$:

$$vC = \frac{C_{conv} - C_{ATES}}{\sum_{i=1}^{n} V_{h,i} + V_{c,fc,i} + V_{c,hp,i}} \tag{19}$$

We note that this analysis focuses on operational costs only rather than upfront investment costs, given the high variability of fixed costs for ATES across different sites and buildings[7].

Collective performance indicators

The simulated GHG savings Δ_{GHG} $[tCO_2]$ correspond to the difference between the emissions of conventional energy systems and ATES systems, for a given amount of delivered energy:

$$\Delta_{GHG} = GHG_{conv} - GHG_{ATES} \tag{20}$$

As a measure of the efficiency with which subsurface volume is used for thermal storage, these greenhouse gas savings can be expressed in relation to the aquifer volume allocated to ATES wells, using the distance policy d, well screen length L_i [m] and the total nominal storage volume of the wells V_i [m^3/yr]:

$$v_{GHG} = \frac{\Delta_{GHG}}{\sum_{i=1}^{n} \pi d R_{th,i}^2} = \frac{c_{aq}}{c_w} \frac{\Delta_{GHG}}{\sum_{i=1}^{n} \frac{V_i}{L_i}} \tag{21}$$

Finally, cost savings and GHG savings can be related as an equivalent GHG abatement cost α_{GHG} $[EUR/tCO_2]$, which will be negative if cost and GHG savings from ATES are both positive:

$$\alpha_{GHG} = (C_{ATES} - C_{conv})/\Delta_{GHG} \tag{22}$$

References

1. Tomasetta, C., Van Ree, C. & Griffioen, J. Life cycle analysis of underground thermal energy storage. In *Engineering Geology for Society and Territory-Volume 5*, 1213–1217 (Springer, 2015).

2. Vanhoudt, D., Desmedt, J., Van Bael, J., Robeyn, N. & Hoes, H. An aquifer thermal storage system in a Belgian hospital: Long-term experimental evaluation of energy and cost savings. *Energy Build.* **43**, 3657–3665 (2011). URL http://www.sciencedirect.com/science/article/pii/S0378778811004427. DOI 10.1016/j.enbuild.2011.09.040.

3. Bloemendal, M., Olsthoorn, T. & van de Ven, F. Combining climatic and geo-hydrological preconditions as a method to determine world potential for aquifer thermal energy storage. *Sci. The Total. Environ.* **538**, 621–633 (2015). URL http://www.sciencedirect.com/science/article/pii/S0048969715304307. DOI 10.1016/j.scitotenv.2015.07.084.

4. Jaxa-Rozen, M., Bloemendal, M. & Kwakkel, J. Quantifying the potential of Aquifer Thermal Energy Storage (ATES) for energy savings in the built environment (Vienna, 2018).

5. Hardin, G. The Tragedy of the Commons. *Sci.* **162**, 1243–1248 (1968). URL http://www.sciencemag.org/content/162/3859/1243. DOI 10.1126/science.162.3859.1243.

6. Bloemendal, M., Jaxa-Rozen, M. & Olsthoorn, T. Methods for planning of ATES systems. *Appl. Energy* **216**, 534–557 (2018). URL http://www.sciencedirect.com/science/article/pii/S0306261918301958. DOI 10.1016/j.apenergy.2018.02.068.

7. Agterberg, F. *Developing strategic options for the Dutch subsoil energy sector*. Master's thesis, TIAS School for Business and Society (2016).

8. Rostampour, V. & Keviczky, T. Distributed Stochastic Model Predictive Control Synthesis for Large-Scale Uncertain Linear System. *arXiv preprint arXiv:1703.06273* (2017). Bibtex: rostampour2017distributed.

9. Bayer, P., Saner, D., Bolay, S., Rybach, L. & Blum, P. Greenhouse gas emission savings of ground source heat pump systems in Europe: A review. *Renew. Sustain. Energy Rev.* **16**, 1256–1267 (2012). URL http://www.sciencedirect.com/science/article/pii/S1364032111004771. DOI 10.1016/j.rser.2011.09.027.

10. Willemsen, N. Rapportage bodemenergiesystemen in Nederland. Tech. Rep., RVO / IF Technology, Arnhem, The Netherlands (2016).

11. Bonte, M. *Impacts of shallow geothermal energy on groundwater quality*. Doctoral dissertation, Vrije Universiteit Amsterdam, Amsterdam (2013).

12. Calje, R. *Future use of Aquifer Thermal Energy Storage below the historic centre of Amsterdam*. Master's thesis, Delft University of Technology (2010).

13. Hähnlein, S., Bayer, P., Ferguson, G. & Blum, P. Sustainability and policy for the thermal use of shallow geothermal energy. *Energy Policy* **59**, 914–925 (2013). URL http://www.sciencedirect.com/science/article/pii/S0301421513002930. DOI 10.1016/j.enpol.2013.04.040.

14. Bloemendal, M., Olsthoorn, T. & Boons, F. How to achieve optimal and sustainable use of the subsurface for Aquifer Thermal Energy Storage. *Energy Policy* **66**, 104–114 (2014). URL http://www.sciencedirect.com/science/article/pii/S0301421513011415. DOI 10.1016/j.enpol.2013.11.034.

15. Ostrom, E. A General Framework for Analyzing Sustainability of Social-Ecological Systems. *Sci.* **325**, 419–422 (2009). URL http://www.sciencemag.org/content/325/5939/419. DOI 10.1126/science.1172133.

16. Jaxa-Rozen, M., Kwakkel, J. & Bloemendal, M. The adoption and diffusion of common-pool resource-dependent technologies: The case of aquifer Thermal Energy Storage systems. In *2015 Portland International Conference on Management of Engineering and Technology (PICMET)*, 2390–2408 (2015). DOI 10.1109/PICMET.2015.7273176.

17. Bloemendal, M., Jaxa-Rozen, M. & Rostampour, V. Improved performance of heat pumps helps to use full potential of subsurface space for Aquifer Thermal Energy Storage. In *12th IEA Heat Pump Conference* (2017). Bibtex: bloemendal2017improved bibtex[organization=Stichting HPC 2017].

18. Eurostat. Electricity prices for non-household consumers - bi-annual data. Tech. Rep. Dataset NRG_PC_205 (2018).

19. Eurostat. Gas prices for non-household consumers - bi-annual data. Tech. Rep. Dataset NRG_PC_203 (2018).

20. McKenna, E., Richardson, I. & Thomson, M. Smart meter data: Balancing consumer privacy concerns with legitimate applications. *Energy Policy* **41**, 807–814 (2012). URL http://www.sciencedirect.com/science/article/pii/S0301421511009438. DOI 10.1016/j.enpol.2011.11.049.

21. Véliz, C. & Grunewald, P. Protecting data privacy is key to a smart energy future. *Nat. Energy* 1 (2018). URL https://www.nature.com/articles/s41560-018-0203-3. DOI 10.1038/s41560-018-0203-3.

22. Kabalci, Y. A survey on smart metering and smart grid communication. *Renew. Sustain. Energy Rev.* **57**, 302–318 (2016). URL http://www.sciencedirect.com/science/article/pii/S1364032115014975. DOI 10.1016/j.rser.2015.12.114.

23. Samad, T. & Kiliccote, S. Smart grid technologies and applications for the industrial sector. *Comput. & Chem. Eng.* **47**, 76–84 (2012). URL http://www.sciencedirect.com/science/article/pii/S0098135412002347. DOI 10.1016/j.compchemeng.2012.07.006.

24. Rostampour, V., Ferrari, R., Teixeira, A. & Keviczky, T. Privatized distributed anomaly detection for large-scale nonlinear uncertain systems. *Submitt. to IEEE Transactions on Autom. Control.* (2018).

25. Ma, Y. *et al.* Model predictive control for the operation of building cooling systems. *IEEE Transactions on control systems technology* **20**, 796–803 (2012). Bibtex: ma2012model bibtex[publisher=IEEE].

26. Farahani, S. S., Lukszo, Z., Keviczky, T., De Schutter, B. & Murray, R. M. Robust model predictive control for an uncertain smart thermal grid. In *Control Conference (ECC), 2016 European*, 1195–1200 (2016). Bibtex: farahani2016robust bibtex[organization=IEEE].

27. Patel, N. R., Risbeck, M. J., Rawlings, J. B., Wenzel, M. J. & Turney, R. D. Distributed economic model predictive control for large-scale building temperature regulation. In *American Control Conference (ACC), 2016*, 895–900 (2016). Bibtex: patel2016distributed bibtex[organization=IEEE].

28. Mirakhorli, A. & Dong, B. Occupancy behavior based model predictive control for building indoor climate—A critical review. *Energy Build.* **129**, 499–513 (2016). Bibtex: mirakhorli2016occupancy bibtex[publisher=Elsevier].

29. Rostampour, V. & Keviczky, T. Probabilistic energy management for building climate comfort in smart thermal grids with seasonal storage systems. *arXiv preprint arXiv:1611.03206* (2016). Bibtex: rostampour2016probabilistic.

30. Wilensky, U. NetLogo (1999).

31. Harbaugh, A. W. *MODFLOW-2005, the US Geological Survey modular ground-water model: the ground-water flow process* (U.S. Geological Survey, 2005).

32. Langevin, C. D., Thorne Jr, D. T., Dausman, A. M., Sukop, M. C. & Guo, W. SEAWAT Version 4: a computer program for simulation of multi-species solute and heat transport. Tech. Rep., U.S. Geological Survey (2008).

33. Bakker, M. *et al.* Scripting MODFLOW Model Development Using Python and FloPy. *Groundw.* n/a–n/a (2016). URL http://onlinelibrary.wiley.com/doi/10.1111/gwat.12413/abstract. DOI 10.1111/gwat.12413.

34. Lofberg, J. YALMIP: A toolbox for modeling and optimization in MATLAB. In *Computer Aided Control Systems Design, 2004 IEEE International Symposium on*, 284–289 (2004). Bibtex: lofberg2004yalmip bibtex[organization=IEEE].

35. van Vliet, E. *Flexibility in heat demand at the TU Delft campus smart thermal grid with phase change materials*. Master's thesis, Delft University of Technology (2013).

36. Ananduta, W. W. *Distributed Energy Management in Smart Thermal Grids with Uncertain Demands*. Master's thesis, Delft University of Technology (2016).

37. Rostampour, V., Bloemendal, J. M. & Keviczky, T. A model predictive framework of Ground Source Heat Pump coupled with Aquifer Thermal Energy Storage System in heating and cooling equipment of a building. *12th IEA Heat Pump Conf.* (2017). URL http://resolver.tudelft.nl/uuid:95255ef7-7267-421a-b3ea-7b701c6064d9.

38. Borren, W. Ontwikkeling HDSR hydrologisch modelinstrumentarium – HYDROMEDAH. Deelrapport 1: Beschrijving MODFLOW model. Tech. Rep., Deltares, Utrecht (2009).

39. Gunnink, J. L. Deklaagmodel en geohydrologische parametrisatie voor het beheersgebied van het Hoogheemraadschap "De Stichtse Rijnlanden". Tech. Rep., TNO, Utrecht (2004).

40. KNMI. KNMI'14: Climate Change scenarios for the 21st Century – A Netherlands perspective. Tech. Rep. KNMI WR 2014-01, KNMI, De Bilt, The Netherlands (2014).

41. Van Vuuren, D. P. *et al.* The representative concentration pathways: an overview. *Clim. change* **109**, 5 (2011). Bibtex: van2011representative bibtex[publisher=Springer].

42. KNMI. KNMI Klimaatscenario's Transformatie tijdreeksen KNMI'14 (2014). URL http://climexp.knmi.nl/scenarios_knmi14_form.cgi.

43. Chan, A. L. S. Developing future hourly weather files for studying the impact of climate change on building energy performance in Hong Kong. *Energy Build.* **43**, 2860–2868 (2011). URL http://www.sciencedirect.com/science/article/pii/S0378778811002957. DOI 10.1016/j.enbuild.2011.07.003.

Appendix

R_{th}	2.125		2.25		2.375		2.5		2.75		3.0	
	CS	DS	CS	DS	CS	DS	CS	DS	CS	DS	CS	DS
Thermal eff.	0.972	0.942	0.988	0.957	0.992	0.969	0.991	0.978	0.994	0.994	1.0	1.0
COP	0.978	0.936	1.014	0.954	1.017	0.967	1.009	0.978	0.992	0.994	0.998	1.0
Tot. GHG savings	0.983	0.952	1.002	0.965	1.017	0.974	1.006	0.982	0.998	0.995	1.003	1.0
Spec. GHG savings	1.961	1.898	1.778	1.713	1.621	1.552	1.448	1.413	1.188	1.185	1.002	1.0

Table 2. Performance regret values for idealized case study, relative to DS 3.0 R_{th}.

	Scenario 1 (3.0 Rth)		Scenario 2 (2.5 Rth)		Scenario 3 (2.25 Rth)	
	DSMPC	DS	DSMPC	DS	DSMPC	DS
Thermal efficiency	1.007	1.0	1.001	0.971	0.998	0.941
COP	1.010	1.0	1.015	0.968	1.034	0.949
Total GHG savings	0.990	1.0	1.060	1.159	1.212	1.290
Specific GHG savings	0.990	1.0	1.157	1.265	1.388	1.518

Table 3. Performance values for Utrecht case study with $Q = 1.0$, relative to DS Scenario 1.

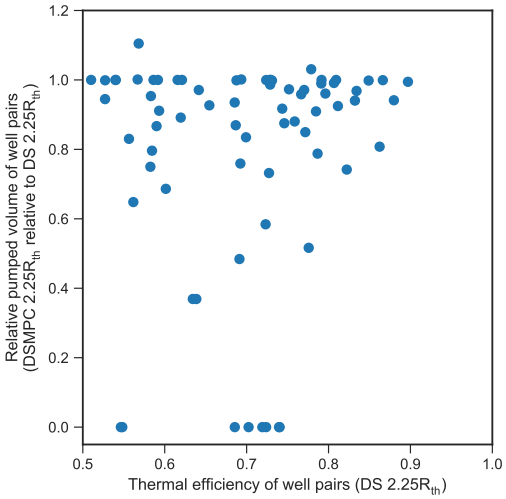

Figure 11. Effect of well coupling constraints on pumped volume for Utrecht case study, as a function of decoupled thermal efficiency in Scenario 3. Each of the markers corresponds to a simulated well pair.